# On the capacity of the underwater acoustic communication channel under realistic assumptions

Jean-Michel Passerieux, François-Xavier Socheleau, Christophe Laot

# On the Capacity of the Underwater Acoustic Communication Channel under Realistic Assumptions

Jean-Michel Passerieux
Thales Underwater Systems
525 route des Dolines, BP 157
06903 Sophia Antipolis Cedex, France.
Email: jean-michel.passerieux@fr.thalesgroup.com

Francois-Xavier Socheleau and Christophe Laot
Institut Telecom; Telecom Bretagne; UMR CNRS 3192 Lab-STICC
Université européenne de Bretagne
Technopôle Brest Iroise-CS 83818, 29238 Brest Cedex, France.
Email: {fx.socheleau, christophe.laot}@telecom-bretagne.eu

***Abstract*—The capacity of the underwater acoustic communications (UAC) channel is addressed under a comprehensive set of assumptions: time-varying multi-paths channel, modelled as a doubly-spread frequency-selective Ricean channel with known statistical properties, actual realization of the channel unkown to the transmitter and receiver, constraints on transmit power (averaged and/or peak) and available frequency bandwidth. The exact channel capacity under such general assumptions is still unknown. Therefore, upper and lower bounds of this capacity are given, and then numerically assessed and discussed for a few typical shallow water UAC channels.**

**It is shown that, as long as the theoretical channel capacity is considered, transmission with spectral efficiency higher than often now (e.g. 2 to 3 bits/sec/Hz) appears as a reasonable objective in typical UAC channels, providing SNR about 15 to 20 dB. In other respects, for a given available averaged transmit power, large peak-to-averaged-power-ratio (PAPR) is also shown to be highly desirable, since it significantly reduces the capacity loss due to the channel uncertainty.**

***Index Terms*—Underwater acoustic communications, channel capacity, doubly selective channel, Rician channel, peak-limited power, PAPR.**

## I. Introduction

This paper is motivated by the increased underwater capability of underwater acoustic communication (UAA) systems that has been experimentally demonstrated in the last few years by applying new modulations and signal processing techniques to UAC. Among these techniques, often borrowed from other domains such as cable or radio communications, the most attractive are likely multi-carriers (MC) modulations (with Orthogonal Frequency Division Multiplex (OFDM) [1], [2] as a special case), efficient channel coding techniques such as turbo or LDPC codes, sparse channel identification [3] and iterative reception algorithms such turbo equalization [4], [5].

Main point is that, even in difficult shallow water environmental conditions, it now appears possible to significantly increase the bitrate with respect to the current state of the art implemented in commercial-on-the-shelf (COTS) modems (e.g. by using modulations having a large number of states, such as 64-QAM, while COTS UAC modems [6], [7] generally use at most QPSK modulations, thus leading, after coding and insertion of pilot signals, to spectral efficiency around 1 bit/sec/Hz).

Therefore, an assessment of the ultimate performance of shallow water UAC, by the means of computation of the Shannon capacity [8], appears critical to determine whether these new techniques could actually yield a significant breakthrough in UAC performance – as it has happened for the last ten years in other domains (wifi, DTV, UWB, etc.). Meanwhile, this interest is also renewed by the outcomes of recent interesting works [9]–[12] on the capacity of fading channels, mainly motivated by the wireless or ultra-wideband (UWB) channels, but which are applicable to the UAC channel as well.

Unlike the capacity of other channels, the capacity of the shallow water UAC channel[1] has been seldomly addressed. Hayward et al. [13] apply a Gaussian-beam propagation code to get the amplitudes and phases of the multipaths in a flat bottom shallow water environment (100 meters depth, range up to 20 km) with an almost unlimited available frequency band (from 100 to $10^6$ Hz). Then, assuming a time-invariant frequency-selective channel, they allocate the transmit power across the available frequency band in order to maximize the channel capacity. Assuming a 193 dB rePa@1 m source level, they eventually get very high theoretical bitrates, about 1 Mbits/sec at 1 km or 100 kbits/sec at 10 km. More recentlty, Stojanovic et al. [14] consider a simpler propagation model (a single path whose signal-to-noise ratio (SNR) at reception varies with frequency and range according to simple acoustic propagation models) and derive approximate simple relations between range, transmit power and channel capacity. Main point is that the works above, even if interesting, are not fully realistic since they neglect some critical characteristics of the UAC channel, its random and highly time-varying impulse response, and of the transmitting devices, the often encountered peak-power and bandwidth limitations.

Hence, this paper is devoted to the capacity of the UAC channel. As often, this channel is modelled as a discrete-

[1]Multiple-inputs multiple-outputs (MIMO) channels are not considered here where the focus is laid upon the single-input single-output (SISO) case.

time Rician-fading single-input single-output (SISO) channels. However, the time-varying multipath propagation leading to selective channels in both time and frequency is considered. Moreover, to provide realistic guidelines for the design of UAC modems, we here study the capacity under several critical assumptions.

- **(A1)** Both peak and average power of the transmitted symbols is limited.
- **(A2)** Neither the transmitter nor the receiver know the current realization of the channel but both know the channel distribution.
- **(A3)** The available frequency bandwidth is limited.

**(A1)** is the direct translation of physical limitations imposed by the transmitting devices (power amplifier, transducer, matching unit) and/or the available power supply. This assumption is fundamental since it rules out the often used Gaussian or 'peaky' signals [15], [16] from the set of capacity achieving inputs. **(A2)** corresponds to the noncoherent setting where the channel state information (CSI) is unknown to both the transmitter and the receiver. Finally, **(A3)** results from obvious physical limitations of transmitting devices.

The main contributions of this paper are threefold:

- Based upon the chain rule [8] and a generalization of the entropy power inequality detailed in [17], lower and upper bounds on noncoherent capacity under peak-power constraint are given for Rician fading channels.
- By applying these bounds to a few simple idealized channels, it is shown that the lack of knowledge on the actual channel realization results in a capacity loss which is strongly dependent upon the Rice factor and the Doppler spread, but also, in a less intuitive manner, upon the peak-to-average power ratio (PAPR).
- These bounds are then applied to real underwater acoustic channels, recorded in the Mediterranean sea, that are typical examples of doubly dispersive Rician UAC fading channels. Capacity of existing underwater communications systems and the theoretical limits are compared.

This paper is organized as follows. Section II is devoted to the presentation of the system model and the main assumptions. Capacity bounds applicable under the above assumptions are given in section III. Section IV is devoted to applying these bounds to a few idealized simple UAC channels and to discuss influence of the Doppler spread, the Rice factor and the PAPR. In section V, the interest of the capacity bounds is illustrated by applying them to a few typical UAC channels measured at sea. Finally, conclusions are given in section VI.

## II. System model

### A. Notation

Throughout this paper, lowercase boldface letters denote vectors, e.g. $\boldsymbol{x}$, and uppercase boldface letters denote matrices, e.g., $\boldsymbol{A}$. The superscripts $^T$ and $^\dagger$ stand for transposition and Hermitian transposition respectively. $\mathcal{CN}(\boldsymbol{m}, \boldsymbol{R})$ stands for the distribution of a jointly proper Gaussian random vector with mean $\boldsymbol{m}$ and covariance matrix $\boldsymbol{R}$. Finally, $\mathbb{E}\{.\}$ stands for expectation.

### B. Channel model

Let $\boldsymbol{x} = [x_0, \cdots, x_{N-1}]^T$ denote the vector of input symbols. These symbols are assumed identically independent distributed (i.i.d.) with the following constraints

$$|x_n|^2 \leq \Omega_x^2, \tag{1}$$

$$\mathbb{E}\left\{|x_n|^2\right\} = \sigma_x^2 \leq \frac{\Omega_x^2}{\beta}, \tag{2}$$

where the peak-to-average power ratio (PAPR) $\beta$ is a constant satisfying $\beta \geq 1$ . The channel output $\boldsymbol{y}$ is given by

$$\boldsymbol{y} = \boldsymbol{H}\boldsymbol{x} + \boldsymbol{w} \tag{3}$$

where $\boldsymbol{w} \sim \mathcal{CN}(0, \sigma_w^2 \boldsymbol{I}_N)$, $\boldsymbol{H}$ is the $N \times N$ proper Gaussian random channel matrix defined as

$$\boldsymbol{H} \triangleq \begin{pmatrix} h_{0,0} & 0 & \dots & \dots & \dots & 0 \\ \vdots & h_{1,0} & \ddots & & & \vdots \\ h_{L-1,L-1} & \vdots & \ddots & \ddots & & \vdots \\ 0 & h_{L,L-1} & & h_{L,0} & \ddots & \vdots \\ \vdots & \ddots & \ddots & \vdots & \ddots & 0 \\ 0 & \dots & 0 & h_{N-1,L-1} & \dots & h_{N-1,0} \end{pmatrix}, \tag{4}$$

and $h_{n,k}$ is the gain at time $n$ of the channel tap $k$, for $n \in [0, N-1]$ and $k \in [0, L-1]$, $L$ designating the length of the channel impulse response. It is also convenient to denote by $\boldsymbol{h}_k = [h_{0,k}, h_{1,k}, \cdots, h_{N-1,k}]^T$ the $N \times 1$ vector corresponding to the $k$-th tap of the channel (i.e. the $k$-th subdiagonal of the channel matrix $\boldsymbol{H}$).

Our channel model relies on the widely used wide-sense stationary uncorrelated scattering (WSSUS) assumption [18], so that

$$\mathbb{E}\{\boldsymbol{h}_k\} = \bar{h}_k \cdot \boldsymbol{1}_N \triangleq \bar{\boldsymbol{h}}_k \tag{5}$$

$$\mathbb{E}\left\{\left[\boldsymbol{h}_k - \bar{\boldsymbol{h}}_k\right]\left[\boldsymbol{h}_l - \bar{\boldsymbol{h}}_l\right]^\dagger\right\} \triangleq \boldsymbol{R}_H(k) \cdot \delta_{k,l} \tag{6}$$

where $\bar{h}_k$ and $\boldsymbol{R}_H(k)$ are the mean and the covariance matrix of the $k$-th channel tap, respectively. For commodity, we denote by $\sigma_h^2(k)$ the element[2] of the main diagonal of $\boldsymbol{R}_H(k)$, and

$$\Xi_H^2 \triangleq \sum_{k=0}^{L-1} \sigma_h^2(k) \tag{7}$$

$$\Psi_H^2 \triangleq \sum_{k=0}^{L-1} |\bar{h}_k|^2 = \int_{-1/2}^{1/2} |\psi_H(\theta)|^2 \, d\theta, \tag{8}$$

where $\psi_H(\theta)$ is the discrete Fourier transform of the mean of the channel impulse response (CIR), i.e., $\psi_H(\theta) = \sum_k \bar{h}_k e^{-2j\pi\, k\, \theta}$.

We also denote by $\mathcal{R}_H$ the sum over the channel taps of the covariance matrices $\boldsymbol{R}_H(k)$, i.e. $\mathcal{R}_H \triangleq \sum_k \boldsymbol{R}_H(k)$, and

[2]Note that, thanks to the WSSUS assumption, the matrix $\boldsymbol{R}_H(k)$ is Toeplitz.

by $\check{\mathcal{S}}_H(\nu)$, the normalized Doppler spectrum of this equivalent time-varying flat-fading channel

$$\check{\mathcal{S}}_H(\nu) = \frac{1}{\Xi_H^2} \sum_{n=0}^{N-1} [\mathcal{R}_H]_{n,1}\, e^{-2j\,\pi\,n\,\nu/N}. \tag{9}$$

Using the above quantities, we can now define the peak SNR of a global equivalent time-varying flat fading channel

$$\mathrm{SNR}_{\mathrm{peak}} \triangleq \Omega_x^2\, \frac{\Psi_H^2 + \Xi_H^2}{\sigma_w^2}, \tag{10}$$

as well as the maximum average SNR

$$\mathrm{SNR}_{\mathrm{av}} \triangleq \frac{1}{\beta}\mathrm{SNR}_{\mathrm{peak}}. \tag{11}$$

Finally, the Rice factor of the $k$-th channel tap is defined as

$$\kappa_k \triangleq \frac{|\bar{h}_k|^2}{\sigma_h^2(k)}. \tag{12}$$

## III. Capacity bounds

As already mentioned, the non coherent case is considered here, where only the statistical properties of the channel are assumed to be known to the transmitter and the receiver, while the actual channel realization is unkown. Hence, with the above notations, the channel capacity [8] is given by

$$C = \lim_{N\to\infty}\ \frac{1}{N}\left[\ \sup_{p_{\boldsymbol{x}}\in\mathcal{P}_{\boldsymbol{x}}}\ I(\boldsymbol{y};\boldsymbol{x})\ \right] \tag{13}$$

where $I(\boldsymbol{y};\boldsymbol{x}) = h_E(\boldsymbol{y}) - h_E(\boldsymbol{y}|\boldsymbol{x})$ is the mutual information between $\boldsymbol{y}$ and $\boldsymbol{x}$, $h_E(\boldsymbol{y})$ the differential entropy of $\boldsymbol{y}$, and the sup is taken for $p_{\boldsymbol{x}}$ in the set $\mathcal{P}_{\boldsymbol{x}}$ of the input symbol distributions which meet the constraints (1) and (2).

### A. Upper bound

Let us first notice that using the chain rule for the mutual information, a rather intuitive bound can be derived[3]. This upper bound, given in theorem 1, corresponds to the ideal assumption where the receiver knows each channel realization and where the input symbols are not peak constrained.

*Theorem 1:* The capacity of a discrete-time Ricean WSSUS channel with i.i.d. input symbols and a peak-power constraint in the time domain is upper-bounded as $C_{\mathrm{coh}}^{\mathrm{DS}}$, where

$$C_{\mathrm{coh}}^{\mathrm{DS}} = \lim_{N\to\infty} \frac{1}{N}\mathbb{E}_{\boldsymbol{H}}\left\{\log\det\left(\boldsymbol{I}_N + \frac{\Omega_x^2}{\beta\,\sigma_w^2}\boldsymbol{H}\boldsymbol{H}^\dagger\right)\right\}. \tag{14}$$

$C_{\mathrm{coh}}^{\mathrm{DS}}$ corresponds to the coherent capacity of the channel $\boldsymbol{H}$ without any restriction on the peak power of the input symbols and with an average SNR equals to $\mathrm{SNR}_{\mathrm{peak}}/\beta$.

[3]Rigorous proofs of the two bounds of section III-B are given in [19]. Note also that, to the best of our knowledge, no closed-from expression is known for the expectation in the right hand side terms of (14) and (15). However, these terms can easily be assessed numerically via a Monte-Carlo technique.

### B. Lower bound

Using the generalization of the entropy power inequality detailed in [17], a lower bound on the channel capacity is given in the following theorem.

*Theorem 2:* The capacity of a discrete-time Rician WSSUS channel with i.i.d. input symbols and a peak-power constraint in the time domain is lower-bounded as $C \geq L_{\mathrm{peak}}^{\mathrm{DS}}$, where

$$L_{\mathrm{peak}}^{\mathrm{DS}} = \lim_{N\to\infty} \frac{1}{N}\mathbb{E}_{\boldsymbol{H}}\left\{\log\det\left(I_N + \lambda\frac{\Omega_x^2}{\beta\,\sigma_w^2}\,\boldsymbol{H}\boldsymbol{H}^\dagger\right)\right\} - \int_{-1/2}^{1/2} \log\left(1 + \frac{\Omega_x^2\,\Xi_H^2}{\beta\,\sigma_w^2}\,\check{\mathcal{S}}_H(\nu)\right) d\nu. \tag{15}$$

$\lambda$ is a weighting factor given by

$$\lambda = \begin{cases} 2\beta/(\pi e), & \text{if } 1 \leq \beta \leq 3 \\ e^{\gamma\Omega_x^2/\beta}\beta/(\pi e K^2\,\Omega_x^2), & \text{if } \beta > 3, \end{cases} \tag{16}$$

where $K$ and $\gamma$ are the solution of the following system of equations

$$\begin{aligned} \int_{-\frac{\Omega_x}{\sqrt{2}}}^{\frac{\Omega_x}{\sqrt{2}}} K e^{-\gamma u^2} du &= 1, \\ \int_{-\frac{\Omega_x}{\sqrt{2}}}^{\frac{\Omega_x}{\sqrt{2}}} u^2 K e^{-\gamma u^2} du &= \frac{\Omega_x^2}{2\beta}, \end{aligned} \tag{17}$$

which can be solved numerically.

It is worth noticing that the lower bound $L_{\mathrm{peak}}^{\mathrm{DS}}$ is the difference of two terms.

- The first term is the coherent capacity of the channel without peak-power limitation as presented above in Theorem 1, but with a SNR loss expressed by the factor $\lambda$. This loss takes into account for the effect of the peak-power constraint. It is plotted Figure 1 below with respect to the PAPR. Note that for $\beta = 0$ dB, the expression of $\lambda$ simplifies to $\lambda = 2/(\pi e)$ which corresponds to a 6.3 dB SNR loss. Then, for increasing $\beta$, the loss decreases until $\beta = 3$, and remains close to 2 dB for $\beta$ above 3.

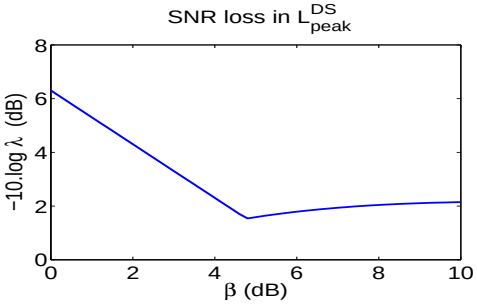


Fig. 1. Equivalent averaged SNR loss versus PAPR $\beta$, as expressed by the first term of the lower bound $L_{\mathrm{peak}}^{\mathrm{DS}}$.

- The second term is a penalty term which corresponds to the capacity loss induced by the channel uncertainty. By inspecting (15), it is easy to see that this second term depends only upon the random part of the CIR. Thus, for

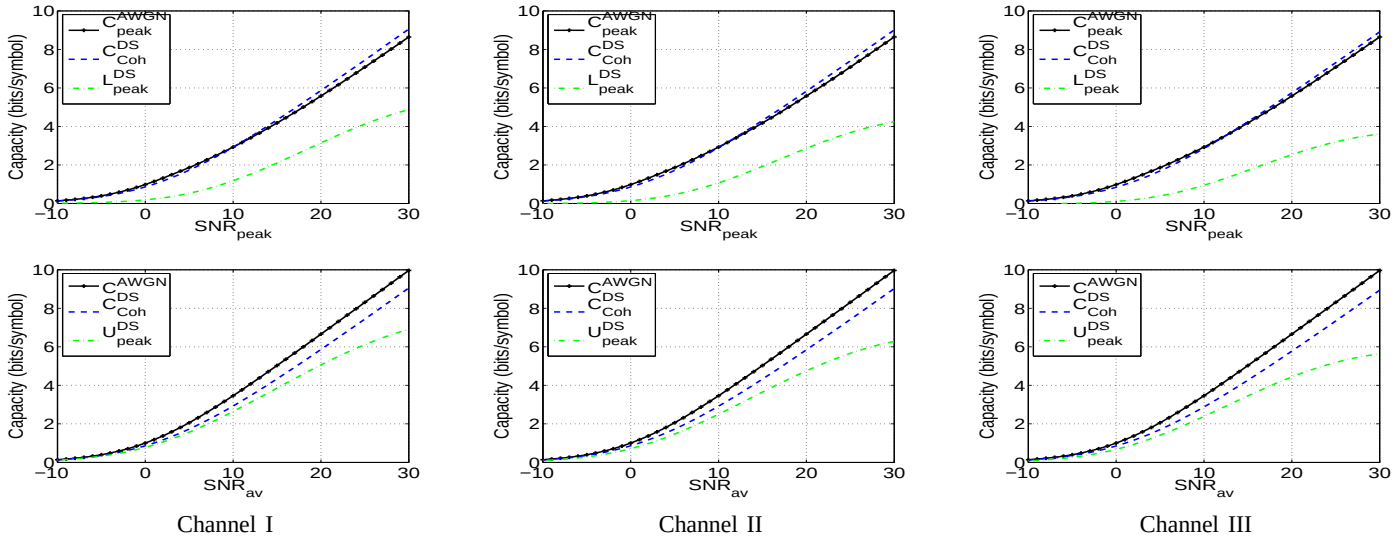


Fig. 2. Capacity bounds for the three idealized channels of Table I. The doppler spread has been taken equal to $0.02/T_s$ (where $T_s$ is the symbol duration)

a given SNR and PAPR, it decreases with the Rice factor and increases with the Doppler spread.

## IV. Application to simple idealized channels

To illustrate the interest of the above bounds, we consider now three simple doubly selective channels whose main parameters (number of paths, power density profile, Rice factors) are given on the table I. For the three channels, the Doppler spread $\mu_{\rm dopp}$ has been taken equal to $0.02/T_s$ (where $T_s$ is the sampling rate). Then, the Doppler profile $\check{S}_H(\nu)$ has been determined from $\mu_{\rm dopp}$ using the maximum entropy derivation proposed in [20]. Moreover, two different situations are considered, characterized by two values of the PAPR: $\beta = 0$ (peak-power constraint only) or $\beta = 10$ (almost pure average-power constraint).

| | paths | delay ($T_s$) | power (dB) | Rice factor |
|---|---|---|---|---|
| | 4 | 0 2 5 10 | 0 -3 -6 -6 | 30 10 5 5 |
| II | 4 | 0 2 5 10 | 0 -3 -6 -6 | 10 5 0 0 |
| III | 4 | 0 2 5 10 | 0 -3 -6 -6 | 5 0 0 0 |

TABLE I
Main parameters for the simple idealized channels

The first situation ($\beta = 0$ dB) corresponds to the case where the transmit power is mainly limited by the cost and volume of the transmitting device which mostly induces a strong constraint on the peak-power. The corresponding capacity bounds are given for the three channels on the first row of Figure 2. As a reference, the capacity $C_{\rm peak}^{\rm AWGN}$ of the peak-limited AWGN channel [21] is also plotted. It can be noticed that the upper bound $C_{\rm coh}^{\rm DS}$ is very close to this capacity $C_{\rm peak}^{\rm AWGN}$. In other respects, these plots clearly show that, even if the unknown theoretical non coherent capacity is likely significantly lower than the capacity $C_{\rm peak}^{\rm AWGN}$, it should remain larger than the bitrate of existing high data rate modems (for instance, 2 to 3 bits/sec/Hz for SNR in the 15-20 dB range, vs typically at most 1 bit/sec/Hz for existing modems).

The second situation is also interesting since it corresponds to the case where the main limitation results from overheating problems of the transmitting device during long continuous transmissions. In this context, it is reasonable to assume that the acoustic transducers cannot usually handle an average power higher than 10% of the allowable peak power ($\beta = 10$ dB). As a reference, the capacity $C_{\rm av}^{\rm AWGN}$ of the AWGN channel without peak limitation is also plotted. By inspecting the corresponding plots, given on the second row of Figure 2, it can be noticed that, in these conditions, the theoretical capacity is also reduced by the doubly dispersive nature of the channel, but in a less significant manner as in the peak-power constraint situation.

The influence of the PAPR $\beta$ is highlighted Figure 3 where the bounds $C_{\rm coh}^{\rm DS}$ and $L_{\rm peak}^{\rm DS}$ are plotted versus $\beta$. We have considered the channel II of table I. The SNR (peak or averaged) and the doppler spread $\mu_{\rm dopp}$ have been set to 15 dB and $2.10^{-2}/T_s$, respectively. It can be observed that in both cases (peak or averaged SNR), providing a PAPR larger than 7 dB, the bounds $C_{\rm coh}^{\rm DS}$ and $L_{\rm peak}^{\rm DS}$ are very close.

In other respects, the influence of the doppler spread $\mu_{\rm dopp}$ is illustrated Figure 4 where the two bounds $C_{\rm coh}^{\rm DS}$ and $L_{\rm peak}^{\rm DS}$ are plotted versus $\mu_{\rm dopp}$. For these plots, the channel II is selected, the averaged SNR is set to 15 dB and two values of the PAPR are considered ($\beta = 0$ or 10 dB). It can be observed that, even for very large (and maybe unrealistic) values of the doppler spread $\mu_{\rm dopp}$, the lower bound $L_{\rm peak}^{\rm DS}$ is significantly less affected for large value of the PAPR $\beta$ than for $\beta$ = 0 dB.

## V. Application to channels measured at sea

We now consider three UAC channels, recorded in the Mediterranean sea off La Ciotat (FR) at a carrier frequency of 6 kHz in a 1 kHz bandwidth, and for three transmission

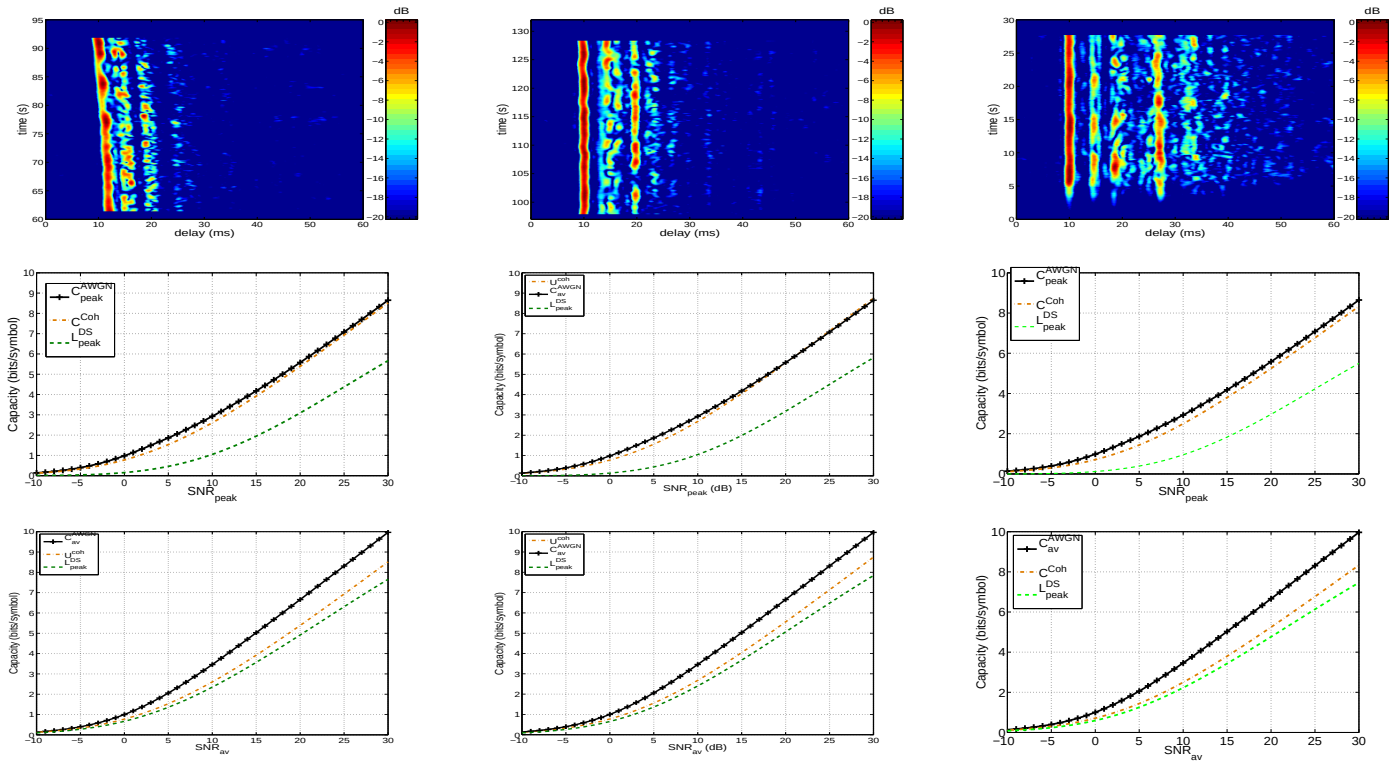


Range 1000 m Range 2500 m Range 5000 m

Fig. 5. Real doubly dispersive Rician fading channel recorded in the Mediterranean sea at three ranges. From top to bottom: channel impulse response versus delay and time ; channel capacity bounds vs peak SNR (dB) for $\beta = 0$ dB ; channel capacity bounds vs averaged SNR (dB) for $\beta = 10$ dB.

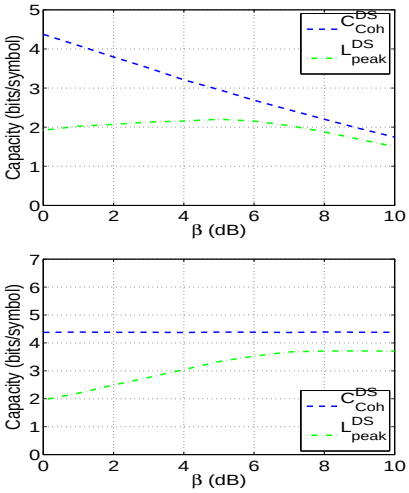


Fig. 3. Capacity bounds $C_{\rm coh}^{\rm DS}$ and $L_{\rm peak}^{\rm DS}$ versus PAPR. Top: constant $\mathrm{SNR}_{\rm peak}$ (15 dB) ; bottom: constant $\mathrm{SNR}_{\rm av}$ (15 dB). Note that the upper bound $C_{\rm coh}^{\rm DS}$ depends upon $\mathrm{SNR}_{\rm av}$ and is independent from the PAPR, while the lower bound $L_{\rm peak}^{\rm DS}$ mainly depends upon $\mathrm{SNR}_{\rm peak}$ and remains almost constant when the PAPR $\beta$ varies within the range 0-10 dB.

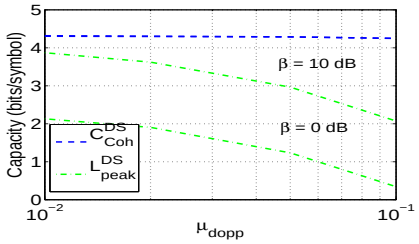


Fig. 4. Capacity bounds versus Doppler spread. Channel II has been selected and averaged SNR set to 15 dB. Note that the upper bounds $C_{\rm coh}^{\rm DS}$ for $\beta = 0$ and $\beta = 10$ are almost indistinguishable for this setting of parameters.

distances, 1000, 2500 and 5000 m. These channels are not as demanding as the most difficult channels of section IV. However, they are typical of the UAC channels frequently encountered in the Mediterranean sea near the continental slope, with a 60 to 120 m water depth.

The corresponding measured channel impulse responses are plotted on the first row of Figure 5. The $\sigma_h^2(k)$ and the $\bar{h}_k$ of (7) and (8), needed to compute the capacity bounds, are estimated using the empirical mode decomposition method as detailed in [22]. For the three channels, the rms Doppler and delay spread have been estimated and and the overall spreading factor found about $10^{-2}$. $\hat{\mathcal{S}}_H(\nu)$ is obtained using the Welch's averaged, modified periodogram spectral estimation method (see the spectrum.welch function of MATLAB). As in section IV, two situations are considered for the PAPR ($\beta$ = 0 or $\beta$ = 10 dB).

As above, the first situation ($\beta = 0$ dB) corresponds to the case where the transmit power is mainly limited by the cost and volume of amplifier. The capacity bounds corresponding to this situation are given by the plots of the second row of the Figure 5. Main observation is that, in spite of the difference between the three considered channels, the plotted upper and lower bounds are very similar for the three considered channels. This can be explained by the strong Rician nature of these channels (for instance, at 2500 m, the Rice factor of the path with a delay $\tau = 10$ ms is around 80).

The third row of Figure 5 shows these capacity bounds in the second situation ($\beta$ = 10 dB). It can be noticed now that, for large SNR, the channel capacity is significantly smaller than the AWGN channel capacity (the difference between these capacities, being roughly equivalent, for $\mathrm{SNR}_{\mathrm{av}} \geq 15$ dB, to a 5 dB loss on the averaged SNR). It can also be observed that, as predicted at the end of section IV (see Fig 3), the bounds $C_{\mathrm{coh}}^{\mathrm{DS}}$ and $L_{\mathrm{peak}}^{\mathrm{DS}}$ are now rather tight. This means that as long as $\beta$ is sufficiently large and $\mu_{\mathrm{dop}}$ relatively small, the knowledge of the channel realizations at the receiver (i.e., a coherent setting) does not bring a significant capacity gain.

Finally, as in section IV, the shape of $L_{\mathrm{peak}}^{\mathrm{DS}}$ in Figure 5 leads to the conclusion that, in the operating SNR range of existing high data rate underwater modems (approx. 15 to 20 dB), these channels should allow to communicate at least at 2 to 3 bits/sec/Hz. This means that, for channels similar to the ones considered here, there is still a significant possible bitrate improvement with respect to existing SISO high data rate modems.

## VI. Conclusion

Upper and lower bounds for the noncoherent capacity of the UAC channel, modelled as a doubly selective Rician fading channels have been presented. A peak-power limitation on the transmit signal (finite PAPR) has been considered to reflect the constraint imposed by electronic devices. The effect of the finite PAPR constraint and of the channel uncertainty induced by the noncoherent setting have been quantified, by an equivalent loss on the averaged SNR and a penalty term that is explicit in the channel Doppler spectrum, respectively. Numerical assessments indicate that, when the peak-to-average power ratio is relatively high ($\geq$ 7 dB), the penalty term remains rather low and the noncoherent setting does not imply a significant capacity loss compared to the coherent setting.

Finally, by studying both very demanding idealized fading channels and real doubly dispersive Rician fading channels, it has been shown that the proposed capacity bounds can provide useful guidelines for future UAC modems development. More precisely, by considering a real underwater acoustic channel, we have shown that in a typical shallow water environment (high Rice factor, channel spreading factor less than $10^{-2}$), there is still a theoretical bitrate gain of a factor 2 to 3 relatively to the existing high data rate underwater modems that usually operate around 1 bit/sec/Hz [6], [7]. Similarly, this also means that there should be a 5 to 10 dB margin between what is implemented today and the ultimate theoretical limits.

## References


[1] M. Chitre, S.H. Ong, and J. Potter, "Performance of coded OFDM in very shallow water channel and snapping schrimp noise," in *Proc. OCEANS 2005, MTS/IEEE*, Brest (FR), June 2005.

[2] F. Frassati, C. Lafon, P.A. Laurent, and J.M. Passerieux, "Experimental assessment of OFDM and DSSS modulations for use in littoral waters underwater acoustic communications," in *IEEE Oceans-Europe 2005*, Brest (FR), June 2005.

[3] C.R. Berger, S. Zhou, J.C. Preisig, and P. Willett, "Sparse channel estimation for multicarrier underwater acoustic communication: From subspace methods to compressed sensing," *IEEE Trans. on Signal Processing*, vol. 38, no. 3, March 2010.

[4] C. Laot, A. Glavieux, and J. Labat, "Turbo equalization: Adaptive equalization and channel decoding jointly optimized," *IEEE Journal on Selected Areas of Commun.*, vol. 19, pp. 1744–1751, Sep. 2001.

[5] R. Otnes and T.H. Eggen, "Underwater acoustic communications: Long-term test of turbo equalization in shallow water," *IEEE Journal of Oceanic Engineering*, vol. 33, no. 3, pp. 321–334, July 2008.

[6] L. Freitag, M. Grund, S. Singh, J. Partan, P. Koski, and K. Ball, "The WHOI micro-modem: an acoustic communications and navigation system for multiple platforms," in *OCEANS, 2005. Proceedings of MTS/IEEE*. IEEE, 2006, pp. 1086–1092.

[7] A.C. Singer, J.K. Nelson, and S.S. Kozat, "Signal processing for underwater acoustic communications," *IEEE Commun. Mag.*, pp. 90–96, Jan. 2009.

[8] T. Cover and J. Thomas, *Elements of Information Theory*, Wiley, 1991.

[9] A. Lapidoth and S.M. Moser, "Capacity bounds via duality with applications to multiple-antenna systems on flat-fading channels," *IEEE Transactions on Information Theory*, vol. 49, no. 10, October 2003.

[10] V. Sethuraman and B. Hajek, "Capacity per unit energy of fading channels with a peak constraint," *IEEE Trans. Inf. Theory*, vol. 51, no. 9, 2005.

[11] M. Gursoy, H.V. Poor, and S. Verdú, "The noncoherent Rician fading channel Part I: Structure of the capacity-achieving input," *IEEE Trans. Wireless Commun*, vol. 4, no. 5, September 2005.

[12] G. Durisi, U.G. Schuster, H. Bölcskei, and S. Shamai (Shitz), "Noncoherent capacity of underspread fading channels," *IEEE Trans. Inf. Theory*, vol. 56, no. 1, 2010.

[13] T. Hayward and T.C. Yang, "Underwater acoustic communication channel capacity: A simulation study," in *Proceeding of AIP Conference*, November 2004, pp. 114–121.

[14] D.Lucani, M.Medard, and M.Stojanovic, "On the relationship between transmission power and capacity of an underwater acoustic communication channel," in *Proc. IEEE Oceans 08 Conference*, Kobe, Japan, April 2008.

[15] I.C. Abou Faycal, M.D. Trott, and S. Shamai (Shitz), "The Capacity of Discrete-Time Memoryless Rayleigh Fading Channels," *IEEE Trans. Inf. Theory*, vol. 47, no. 4, pp. 1290–1301, 2001.

[16] S. Verdu, "Spectral efficiency in the wideband regime," *IEEE Trans. Inf. Theory*, vol. 48, no. 6, pp. 1319–1343, 2002.

[17] R. Zamir and M. Feder, "A generalization of the entropy power inequality with applications," *IEEE Trans. Inf. Theory*, vol. 39, no. 5, Sep. 1993.

[18] P. A. Bello, "Characterization of randomly time-variant linear channels," *IEEE Trans. Commun. Systems*, vol. 11, no. 4, pp. 360–393, 1963.

[19] J.M. Passerieux, F.X. Socheleau, and C. Laot, "On the Noncoherent Capacity of Doubly Selective Rician-Fading Channels under Peak-Power Constraint," *Arxiv preprint arXiv:1011.3380*, 2010.

[20] F.-X. Socheleau, C. Laot, and J.-M. Passerieux, "Concise derivation of scattering function from channel entropy maximization," *IEEE Trans. Commun*, vol. 58, no. 11, Nov. 2010.

[21] S. Shamai (Shitz) and I. Bar-David, "The capacity of average and peak-power-limited quadrature gaussian channels," *IEEE Trans. Inf. Theory*, vol. 41, no. 4, Jul. 1995.

[22] F.-X. Socheleau, J.-M. Passerieux, and C. Laot, "Characterisation of Time-Varying Underwater Acoustic Communication Channel with Application to Channel Capacity," in *Proc. Underwater Acoustic Measurement: Technologies and Results*, Jun. 2009.